2-21-2018

Quantum Dot Growth on (111) and (110) Surfaces Using Tensile-Strained Self-Assembly

Paul J. Simmonds
Boise State University

Publication Information

Simmonds, Paul J. (2018). "Quantum Dot Growth on (111) and (110) Surfaces Using Tensile-Strained Self-Assembly". *Proceedings of SPIE, 10543*, 105430L-1 - 105430L-10. http://dx.doi.org/10.1117/12.2299676

Quantum dot growth on (111) and (110) surfaces using tensile-strained self-assembly

Paul J. Simmonds* [a]

[a] Dept. of Physics / Micron School of Materials Science & Engineering, Boise State University, 1910 University Drive, Boise, ID 83725, USA

ABSTRACT

The self-assembly of epitaxial quantum dots on (001) surfaces, driven by compressive strain, is a widely used tool in semiconductor optoelectronics. In contrast, the growth of quantum dots on (111) and (110) surfaces has historically been a significant challenge. In most cases the strain relaxes rapidly via dislocation nucleation and glide before quantum dots can form. In this paper, we discuss a method for the reliable and controllable self-assembly of quantum dots on both (111) and (110) surfaces, where tensile strain is now the driving force. By showing that tensile-strained self-assembly is applicable to several material systems, we demonstrate the versatility of this technique. We believe that tensile-strained self-assembly represents a powerful tool for heterogeneous materials integration, and nanomaterial development, with future promise for band engineering and quantum optics applications.

Keywords: Tensile strain, quantum dots, self-assembly, (111), (110), fine structure splitting.

1. INTRODUCTION

Since the early 1990s, self-assembled quantum dots (QDs) have been the subject of intensive research for technologies ranging from high-stability lasers, to intermediate band solar cells.[1,2] Under large compressive strains, semiconductor QDs form spontaneously via the Stranski-Krastanov (SK) mechanism on the (001) surfaces of both III-V and group IV materials.[3,4] In zinc-blende and diamond-cubic materials, the shear stress caused by the compressive strain is aligned with the {111} glide plane in such a way that plastic strain relief by dislocation nucleation is energetically unfavorable.[5,6] A window therefore exists within which partial elastic strain relief by 3D roughening takes place instead,[7] resulting in the self-assembly of dislocation-free QDs.

That being said, QDs grown on non-(001) surfaces such as (111) and (110), or QDs grown under *tensile* rather than compressive strain, are highly desirable for certain applications. The low fine-structure splitting of (111) QDs should make them ideal entangled photon sources,[8] while tensile-strain dramatically reduces semiconductor band gaps.[9] The ability to synthesize (111)-oriented and tensile-strained QDs therefore has implications for quantum optics, infrared optoelectronics, and nanoscale band structure engineering. However, until recently it has been enormously challenging to synthesize QDs on (111) and (110) surfaces, or tensile-strained QDs, that are free from strain-related crystallographic defects such as dislocations.[10–13] In both situations, the strain-induced shear stress is aligned with the corresponding {111}glide plane in such a way that the energy barrier to dislocation nucleation and glide is very low.[5,6] As a result, to obtain QD growth on non-(001) surfaces, researchers have resorted to inventive approaches such as droplet epitaxy,[14,15] and growth on pre-patterned substrates.[16,17] Only a few isolated reports of dislocation-free tensile-strained QDs exist.[18–20] Despite the merits of these alternative approaches, a QD self-assembly process based on the single-step SK or Volmer-Weber (VW) mechanisms would be preferable from the points of view of simplicity, scalability, and crystal quality.

To this end, we have pioneered a new, single-step approach based on molecular beam epitaxy (MBE) that enables the self-assembly of dislocation-free, tensile-strained QDs on (111) and (110) surfaces.[5,21–25] The success of this approach comes from recognizing that combining tensile strain *and* a (111) or (110) surface restores the energy barrier to dislocation nucleation and glide. On both the (111) and (110) surfaces, the tensile strain-induced shear stresses align with the respective {111} glide planes to effectively reproduce the situation for compressive strain on a (100) surface.[5,6] As a result, we once again obtain a window where strain relief via QD self-assembly can occur before dislocation formation. The outcome is a

* paulsimmonds@boisestate.edu; phone 1 208 426-3787; fax 1 208 426-4330

Quantum Dots and Nanostructures: Growth, Characterization, and Modeling XV, edited by Diana L. Huffaker, Holger Eisele, Proc. of SPIE Vol. 10543, 105430L · © 2018 SPIE
CCC code: 0277-786X/18/$18 · doi: 10.1117/12.2299676

single-step, tensile-strained self-assembly process that results in the reliable, controllable growth of defect-free QDs on (111) and (110) surfaces.

We have now demonstrated the viability of tensile-strained self-assembly as a new tool for heterogeneous materials integration and nanomaterial development in several materials systems. In this paper, we review the current progress made in this emerging field of optoelectronic nanostructure synthesis, and outline some of the applications for the resulting QDs that take advantage of their unique properties.

2. GaP QD SELF-ASSEMBLY ON GaAs(110) and (111)

2.1 GaP QDs on GaAs(110)

We carried out our initial proof-of-concept studies of tensile-strained self-assembly in the GaP/GaAs(110) material system. The first challenge is that growth of smooth homoepitaxial GaAs(110) buffers is more difficult than on the traditional (001) substrate orientation. The result is frequently material with a very rough surface, and poor electrical and optical properties.[26,27] Nevertheless, these issues can largely be resolved by carefully control of the MBE parameters during growth, namely by selecting low growth rates, high V/III ratios, and low substrate temperatures.[6,28–30]

We then deposited GaP onto the smooth GaAs(110) buffers to test our hypothesis that dislocation-free self-assembly would occur.[21] Due to its smaller lattice constant, GaP on GaAs experiences 3.7% tensile strain. We found that this tensile-strain causes the GaP to self-assemble into QDs (Fig. 1). Transmission electron microscopy (TEM) reveals that below some size threshold (~6 ML), the self-assembled GaP QDs are dislocation-free, as predicted.[21] We can readily tune QD size and areal density by adjusting the amount of GaP we deposit (Fig. 1).[21]

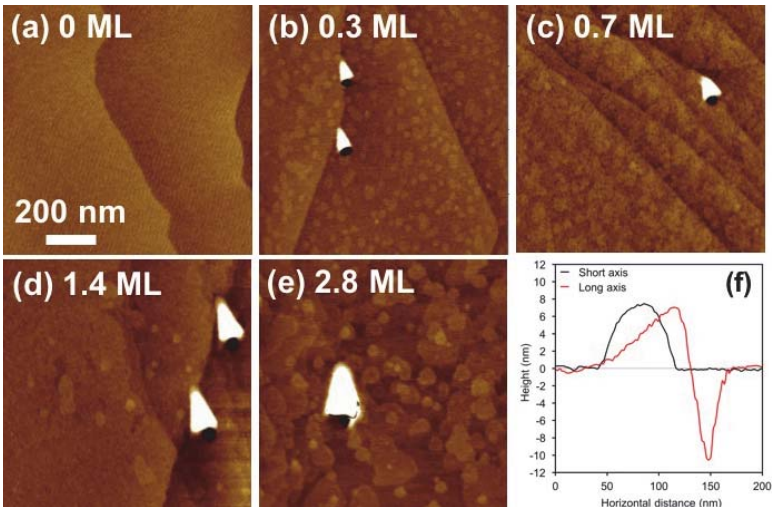

Figure 1. 1×1 μm^2 atomic force micrographs, showing the evolution of GaP/GaAs(110) QDs with GaP deposition amount (z-scale is 3 nm). (a) After 0 ML(monolayers) of GaP (i.e., the bare GaAs(110) buffer surface), and (b)–(e) with GaP deposition increasing from 0.3–2.8 ML. (f) Line sections taken along the long and short axes of the 0.7 ML QD shown in (c).

These GaP(110) QDs exhibit some interesting features. In archetypal compressively strained QD systems, such as InGaAs/GaAs(001), the dots are typically quasi-circular dots in shape.[3] In contrast, the GaP(110) QDs in Fig. 1 adopt a distinctive, conical shape, with a constant length/width ratio of ~2 for all samples. The axis of symmetry of these QDs is consistent across samples, aligned along the $[\bar{1}1\bar{1}]$ direction. Interestingly, each GaP(110) QD is also accompanied by a nanohole located at the "base" of the cone. This can be most clearly seen in the long-axis line section in Fig. 1(f). QDs with very similar line profiles have been previously reported for the InGaAs/GaAs QDs grown by droplet epitaxy on the (311)A surface.[31] The most likely mechanism for nanohole formation is the out-diffusion of arsenic and etching of the underlying buffer material by gallium-rich surface droplets.[32]

Rather than forming via the SK mechanism that is typical for compressive (001) QDs, the GaP(110) QDs form via the VW growth mode. Self-assembled GaP(110) QDs are clearly evident even when significantly less than one monolayer of material has been deposited (Fig. 3(b)). This observation precludes the formation of a continuous 2D wetting layer prior

to the onset of 3D QD formation, which is the signature of SK growth.[3] The fact that we see VW rather than SK growth is likely a function of the surface energies of the GaP/GaAs system.[21]

The QDs have very low areal density of ~7×10^7 cm^{-2}. Regardless of deposition amount, the size distribution of GaP(110) QDs is monomodal, with no evidence of Ostwald ripening.[21] We attribute the low areal density and uniformity of the GaP(110) QDs to the fact that adatom migration lengths are much longer on (110) surfaces than on (001).[33] Gallium adatoms can therefore be efficiently shared between the growing QDs, and could result in QDs reaching an equilibrium size, a phenomenon that has been proposed but rarely observed in traditional (001) QDs.[34] Another feature that results from the high adatom mobility of (110) surfaces is that fact that the GaP QDs nucleate solely at step-edges on the surface. This contrasts with compressive (001) QDs that tend to nucleate randomly across the surface. The longer migration length on (110) means Ga adatoms are able to reach the very low energy sites available at the step edges before QD nucleation begins.[5]

2.2 GaP QDs on GaAs(111)A

Having verified our model for (110) surfaces, we moved on to test the prediction that tensile-strained self-assembly should also occur on (111)-oriented surfaces. We began by optimizing the growth of homoepitaxial buffers on GaAs(111)A substrates (i.e., the gallium-terminated surface orientation). The primary challenge for growth on (111)A is the formation of pyramidal surface defects that appears to be linked to the low sticking coefficient of arsenic on these surfaces.[35,36] Therefore, by using very large V/III ratios to avoid arsenic-limited growth, we are able to grow reasonably smooth GaAs(111)A buffers.[22]

Depositing tensile-strained GaP onto these GaAs(111)A buffers results in QD self-assembly. As before, TEM analysis shows that these GaP(111)A QDs are free from dislocations and coherently strained to the GaAs buffer.[22] This time the GaP QDs resemble equilateral triangles, reflecting the three-fold symmetry of the (111) surface. As we saw for the GaP(110) QDs, growth of the GaP(111)A QDs proceeds via the VW growth mode. As expected, we can tune QD size by increasing the amount of GaP deposited. We can also control QD size and areal density by adjusting the substrate temperature during GaP deposition (Fig. 2). Raising the substrate temperature from 520–580 °C, increases average QD height (from 3-7 nm) and radius (from 40-83 nm), while decreasing the areal density (from $2 \times 10^9 - 7 \times 10^8$ cm^{-2}). Ga adatom diffusion length rises as we increase the substrate temperature, resulting in the formation of low density, larger dots that minimize strain energy more efficiently than numerous small dots.[37]

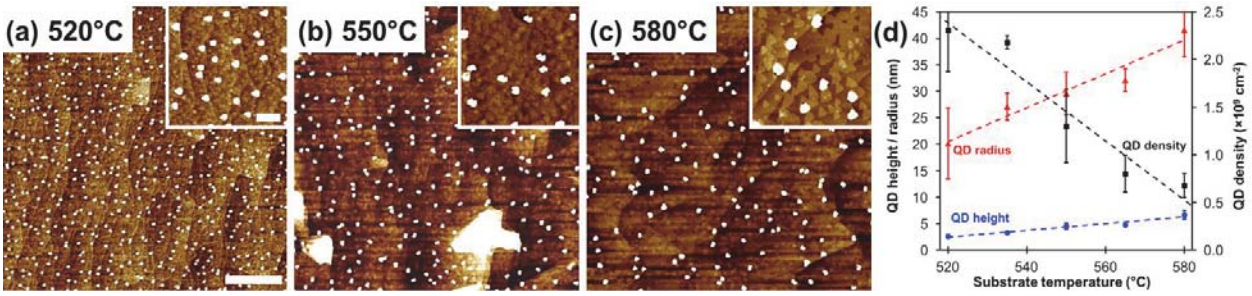

Figure 2. (a)–(c) 5×5 μm^2 atomic force micrographs, showing the evolution of GaP/GaAs(111)A QDs with substrate temperature during GaP deposition (scale bar is 1 μm, z-scale is 3 nm). Insets show higher magnification 1×1 μm^2 images of each sample (scale bar is 200 nm, z-scale is 3 nm). (d) Summary of GaP QD size and areal density statistics as a function of substrate temperature. As substrate temperature is raised, average QD height and size increase, while QD density reduces.

Growth of GaP(111)A QDs obeys island scaling theory.[22] We see an increase in the critical cluster size for QD nucleation as we raise the substrate temperature, compatible with nucleation behavior in other material systems.[38,39] This agreement indicates that the kinetics underpinning tensile-strained self-assembly of GaP(111)A QDs are consistent with what has been established for traditional compressive QD self-assembly.

There are some key differences between the GaP(110) and GaP(111)A QDs. GaP(111)A QDs nucleate randomly across the GaAs surface, rather than only at the step-edges like the GaP(110) QDs. In addition, the areal densities of the GaP(111)A QDs are at least an order of magnitude higher than the 7×10^7 cm^{-2} we observe for the GaP(110) QDs.[21] We can explain both of these differences by the fact that Ga adatom mobility is lower on (111)A than (110) surfaces.[33] Adatoms hence do not have enough energy to reach the closest step-edges, and instead QD nucleation occurs closer to where the adatoms first land on the surface. The result is a higher density of randomly distributed QDs on the (111)A surface.

2.3 GaP quantum wires on GaAs(111)B

To complete this initial study of tensile-strained self-assembly on low-index, non-(001) planes, we moved to the GaAs(111)B surface (i.e., the arsenic-terminated surface orientation). Growth of smooth GaAs with a (111)B orientation is notoriously difficult, with the surface typically covered in wide, short triangular defects composed of three vicinal (111) facets inclined at ~2° from the surface.[40] It is possible to suppress growth on these facets by using misoriented substrates, offcut by 2° in the $\langle 2\bar{1}\bar{1} \rangle$ direction.[40] The outcome is growth of smooth GaAs(111)B buffers whose surface morphology is dominated by terraces around 50 nm wide that result from the offcut (Fig. 3(a)). The terraces are separated by step-bunches ~6 ML in height.

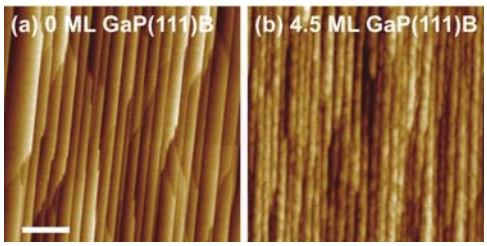

Figure 3. 1×1 μm^2 atomic force micrographs, showing the surface morphology of GaAs(111)B buffers (a) before and (b) after 4.5 ML of GaP deposition (scale bar is 200 nm, z-scale is 3 nm).

When GaP is deposited onto these GaAs(111)B buffers, it too undergoes tensile-strained self-assembly, just as we see for GaP(110) and GaAs(111)A.[5] The difference in this situation is that the morphology of the resulting GaP(111)B nanostructures conforms to that of the underlying GaAs buffer. During GaP deposition, Ga adatoms landing on a given terrace are prevented from moving up or down to neighboring terraces due to the potential barriers caused by the steep step-bunches. The only direction in which the adatoms can therefore move is along the terraces. The result is the formation of tensile-strained 1D GaP quantum wires instead of discrete QDs. These 4.5 ML GaP(111)B quantum wires are ~2 nm high and typically several microns long. Their width is dictated by the width of the underlying GaAs(111)B terraces.[5]

2.4 Summary of GaP QD self-assembly on GaAs(110) and (111)

The results described in the preceding three sections verify that our model for tensile-strained self-assembly is correct. When tensile-strained zinc-blende GaP is deposited onto a (110)- or (111)-oriented surface, partial elastic strain relief by surface roughening takes place before the onset of plastic strain relief by dislocation nucleation and glide. The result is the spontaneous formation of defect-free 3D nanostructures by the VW growth mode, the features of which are dominated by Ga adatom mobility on each GaAs buffer surface orientation. We can readily tune the size and areal density of the GaP nanostructures both by controlling the amount of material deposited, and by the MBE growth conditions.

GaP is however an indirect band gap semiconductor, and so these QDs and quantum wires are not optically active. The second stage of tensile-strained self-assembly development was therefore to extend this novel approach to direct band gap semiconductors.

3. GaAs QD SELF-ASSEMBLY ON InAlAs(110) and (111)

We selected tensile-strained GaAs deposited on $In_{0.52}Al_{0.48}As$ buffers for the second stage of our study. $In_{0.52}Al_{0.48}As$ (InAlAs) is lattice matched to InP substrates. We chose this material system for several reasons. First, both GaAs and InAlAs are direct band gap materials, meaning that any tensile-strained nanostructures that form should be optically active. Second, the lattice mismatch between GaAs and InAlAs is almost identical to that between GaP and GaAs, so that these two systems are almost identical from the point of view of the tensile strain. Third, we wanted to find a tensile-strained system where the band gap of the buffer material is greater or equal to that of the nanostructure material. This arrangement is a requirement for carrier confinement within the nanostructures. The GaAs/InAlAs system meets this requirement. Without strain, the band gap of InAlAs is slightly larger than that of GaAs (1.45 eV and 1.42 eV respectively at 300 K). However, we calculate that the band gap of GaAs will shrink by as much as 0.7 eV when the 3.7% tensile strain is taken into account, leading to robust carrier confinement within the InAlAs barriers.[23,24]

3.1 GaAs QDs on InAlAs(110)

Mirroring our approach with the GaP/GaAs experiments, we began with GaAs deposited on InAlAs(110). Growth of smooth InAlAs buffers on non-(001) InP substrates is perhaps even more of a challenge than the GaAs homoepitaxial buffers in Section 2. The fact that the sticking coefficient of indium rapidly reduces at temperatures above 545 °C places a major constraint on the MBE growth conditions that can be used.[41] This is compounded by the fact that the adatom mobility of Al is typically lower than that of Ga. The growth of InAlAs on InP(110) by MBE is the subject of only a small handful of studies.[42–44] Nevertheless, by using extremely low substrate temperatures and high arsenic overpressures it is possible to achieve growth of smooth InAlAs(110) (Fig. 4(a)).[44]

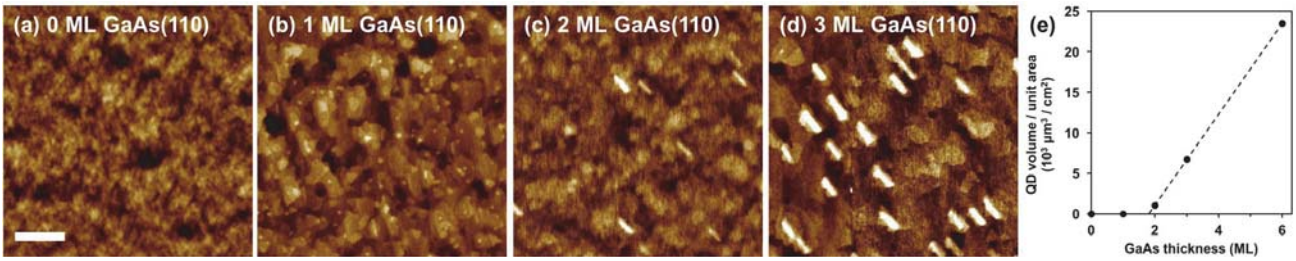

Figure 4. (a)–(d) 1×1 μm^2 atomic force micrographs, showing the evolution of GaAs(110) QD self-assembly as a function of GaAs deposition thickness (scale bar is 200 nm, z-scale is 2 nm). (e) Total volume of GaAs in QDs per unit area as a function of deposition thickness. The linear fit indicates a critical thickness of 1.8 ML for the SK growth transition.

GaAs deposited onto InAlAs(110) initially forms a smooth 2D wetting layer (Fig. 4(b)). However, as the deposition thickness is increased to 2 ML, we see a transition from 2D to 3D growth with the formation of self-assembled GaAs QDs (Fig. 4(c)). This is a critical difference from the GaP QDs above for which we saw VW-based self-assembly at submonolayer deposition thicknesses. Here, the formation of a 2D wetting layer prior to GaAs(110) QD self-assembly is a signature of SK growth. Since the tensile strains experienced by the GaP and GaAs are similar, this change from VW to SK growth is most likely due to the different surface energies of the GaAs/InAlAs system. The GaAs(110) QDs increase in both size and areal density as we raise the deposition thickness further to 3 ML (Fig. 4(d)). After calculating the total volume of material per unit area incorporated into the 3D QDs as a function of GaAs deposition thickness, we can extrapolate back and estimate a critical thickness of 1.8 ML for the 2D to 3D growth transition.

The quasi-rectangular GaAs(110) QDs are elongated in the $[1\bar{1}0]$ direction, with an average aspect ratio of 2.4. Interestingly, we see no evidence of the nanoholes that formed during GaP(110) QD self-assembly (Fig. 1). TEM analysis shows that these tensile-strained QDs are again dislocation-free.[23] High crystalline quality, combined with the direct band gap of the GaAs, means that these tensile strained QDs are optically active (Fig. 5).

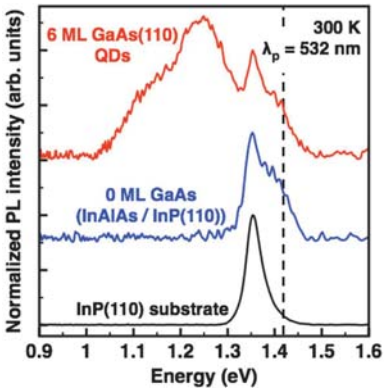

Figure 5. Room temperature PL from a sample containing 6 ML GaAs(110) QDs. Control spectra from the InP(110) substrate and a 0 ML QD sample (i.e., just the InAlAs barriers on InP) are shown for comparison. The dashed line indicates the band gap of bulk GaAs at 300 K. The pump laser wavelength is 532 nm.

GaAs(110) QDs buried under a top InAlAs barrier emit room-temperature photoluminescence (PL) that is readily tunable with QD size because of quantized carrier confinement.[23] Figure 5 shows the PL spectrum for a sample containing 6 ML GaAs(110) QDs, which emit light at 1.24 eV (1000 nm) (Fig. 5). Fundamental to this work is the fact that the GaAs(110)

QD PL is at lower energy than the 300 K band gap of bulk (i.e., unstrained) GaAs at 1.42 eV (873 nm) (dashed line in Fig. 5). This red-shift in the GaAs(110) QD PL is consistent with the presence of tensile strain, and its effect of reducing the semiconductor band gap. Despite the fact that carrier confinement within the QDs pushes the energy states away from the band edges, we still see a net reduction in photon energy of 200 meV compared to bulk GaAs, confirming the dramatic effect of tensile strain on the GaAs QD band structure.

3.2 GaAs QDs on InAlAs(111)A

MBE growth of smooth InAlAs on InP(111)A is not straightforward. We typically see large, 50 nm tall pyramidal defects, with areal densities around 10^7 cm^{-2}, while features consisting of concentric 2D islands appear in the smoother regions between the pyramids.[44] Using high substrate temperature, a low growth rate, and a very high V/III ratio during InAlAs(111)A growth helps to significantly reduce the appearance of these features, but it is not possible to eliminate them completely. We also found that inserting a thin layer of lattice-matched $In_{0.53}Ga_{0.47}As$ between the InAlAs and the InP(111)A substrate led to a marked improvement in surface morphology.[44]

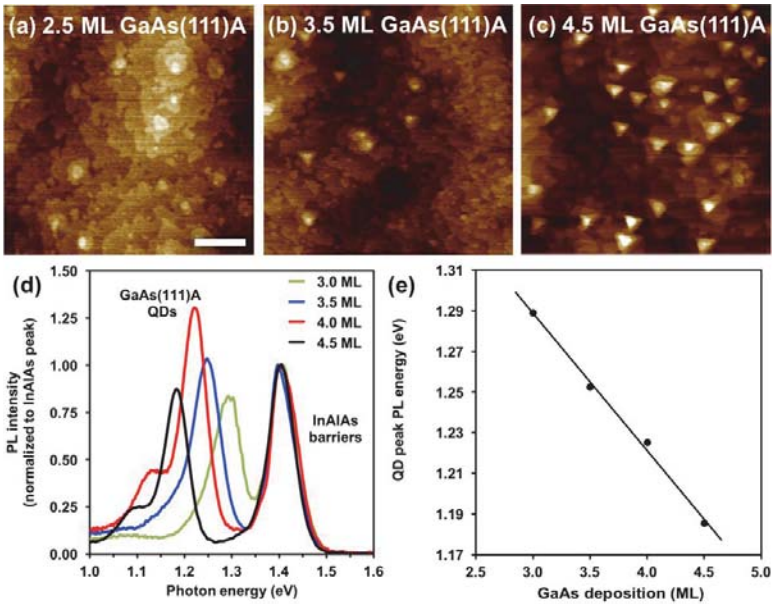

Figure 6. (a)–(c) 1×1 μm^2 atomic force micrographs, showing the evolution of GaAs(111)A QD self-assembly as a function of GaAs deposition thickness (scale bar is 200 nm, z-scale is 2 nm). (d) 7 K PL spectra from (111)A QDs as a function of GaAs deposition thickness in the range 3.0–4.5 ML (spectra normalized to InAlAs barrier peak height). (e) Plot of peak QD PL energy from (d) against GaAs deposition amount.

2.5 ML GaAs deposition results in a smooth, 2D surface (Fig. 6(a)), while by 3.5 ML, a transition to 3D growth occurs, consistent with SK growth. Small GaAs(111)A QDs appear (Fig. 6(b)), which then increase in both size and areal density by 4.5 ML (Fig. 6(c)). The well-resolved triangular shape of the QDs corresponds to the three-fold symmetry of the (111)A substrate. These self-assembled GaAs(111)A QDs are free from dislocations and optically active up to room temperature.[25] PL emission from GaAs(111)A QDs buried under a top InAlAs barrier is highly tunable with QD size over the range 1.18–1.29 eV at 7 K (960–1050 nm) (Fig. 6(d)). We observe the expected redshift as QDs get larger, due to quantum confinement effects (Fig. 6(e)). The linearity of this trend means that we can accurately grow QDs with any emission energy in this range by targeting a given GaAs deposition amount. Once again, due to the large tensile strain, the GaAs(111)A QDs emit light at much lower energy than the band gap of bulk GaAs (1.52 eV at 7 K).

Light emission is most intense for the 4.0 ML GaAs(111)A sample as it has the highest areal QD density, and so the largest number of emitters. We see a low-energy shoulder start to appear on the 3.5 ML QD peak, which develops into a secondary, low-energy peak for the 4.0 and 4.5 ML QD samples. This additional peak indicates emission from a population of larger QDs, suggesting the onset of Ostwald ripening and the development of a bimodal QD size distribution.[45]

3.3 GaAs quantum wires on InAlAs(111)B

As for the GaAs(111)B substrates discussed in Section 2.3, to promote the growth of smooth InAlAs buffers we use InP(111)B substrates offcut by 2° in the $\langle 2\bar{1}\bar{1} \rangle$ direction.[46] The optimal conditions for MBE growth of InAlAs(111)B are a high substrate temperature of 540 °C and a V/III ratio of 10–12.[44]

The InAlAs buffer is smooth, with shallow striations along $[01\bar{1}]$ as a result of the substrate offcut (Fig. 7(a)). Just as for the GaP(111)B, tensile-strained self-assembly takes place via the formation of GaAs(111)B quantum wires that decorate each terrace on the InAlAs buffer surface.[24] The quantum wires grow in both height and width with increasing GaAs deposition (Figs. 7(b)–(c)). Their length is typically on the order of several hundred nanometers.

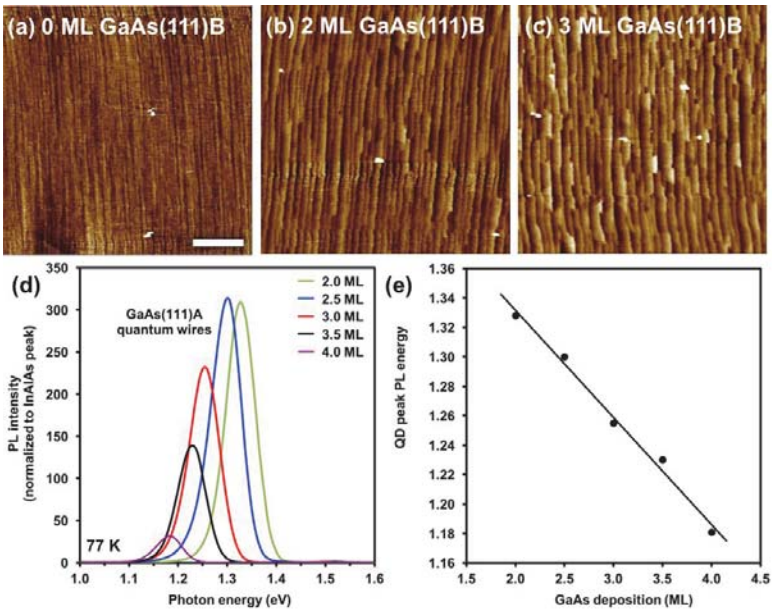

Figure 7. (a)–(c) 1×1 μm^2 atomic force micrographs, showing the evolution of GaAs(111)B quantum wire self-assembly as a function of GaAs deposition thickness (scale bar is 200 nm, z-scale is 3 nm). (d) 77 K PL spectra from (111)B quantum wires as a function of GaAs deposition thickness in the range 2.0–4.0 ML (spectra normalized to InAlAs barrier peak). (e) Plot of peak QD PL energy from (d) against GaAs deposition amount.

The GaAs(111)B quantum wires are defect-free and optically active (Fig. 7(d)).[24] GaAs(111)B quantum wires buried under a top InAlAs barrier offer carrier confinement, since their PL emission energy is once again tunable with GaAs deposition amount, (i.e., quantum wire size). Due to quantum confinement effects, we see the expected redshift over the range 1.33–1.18 eV (932–1051 nm) as the wires get larger (Fig. 7(e)). Again, a linear response means that we can readily tune the quantum wires to any emission energy in this range. The large residual tensile strain in the GaAs(111)B quantum wires mean they emit light below the band edge of bulk GaAs (1.51 eV at 77 K).

Light emission is most intense for the 2 ML GaAs(111)B quantum wire sample. By 4 ML, the accumulated strain has become sufficiently large to overcome the energy barrier to dislocation nucleation and glide.[24] The resulting defects quench the PL from the 4 ML GaAs(111)B quantum wires.

3.4 Summary of GaAs QD self-assembly on InAlAs(110) and (111)

When tensile-strained GaAs is deposited onto a (110)- or (111)-oriented surface, partial elastic strain relief by surface roughening takes place before the onset of plastic strain relief by dislocation nucleation and glide. The result is the spontaneous formation of defect-free quantum dots or wires by the SK growth mode. The size and areal density of the GaAs nanostructures are readily tunable by controlling the amount of material deposited, or the MBE growth conditions.

Since GaAs is a direct band gap semiconductor, these QDs and quantum wires are optically active up to room temperature, indicating strong carrier confinement. We can predictably control their emission wavelength, simply by adjusting their size to take advantage of quantum confinement effects.

In summary, we have established tensile-strained self-assembly as a robust and controllable technique for synthesizing quantum dot and quantum wire nanostructures on the (111) and (110) surfaces of zinc-blende semiconductors. Tensile-strained self-assembly is a general approach that can in principle be applied to any zinc-blende or diamond-cubic material system.

4. NON-(001) TENSILE STRAINED QDs: APPLICATIONS AND FUTURE DIRECTIONS

Tensile-strained self-assembly offers new opportunities for the integration of heterogeneous materials. The resulting quantum dots and wires represent an emerging class of nanostructures in their own right, with certain unique properties that arise either from their non-(001) orientation or from their tensile strain. The future applications we are exploring for these nanostructures therefore seek to take advantage of these distinctive characteristics. QDs grown on (111) surfaces have long been desirable for on-demand entangled photon sources. We have already confirmed that the fine structure splitting between the orthogonal bright exciton states in these QDs is very small, which is a key requirement for robust entanglement.[8,25] Now that we can routinely grow these (111)-oriented QDs via the SK mechanism, the next stage is to develop them as entangled photon emitters.

In parallel to these efforts, the large residual tensile strains in these QDs can also be beneficial. As we have seen, tensile strain pushes the QD towards longer wavelengths, meaning that these nanostructures could be of great interest for infrared optoelectronics, especially if they were synthesized from a low band gap semiconductor. Another way in which we might take advantage of the tensile strain would be to alter the fundamental properties of certain materials via band structure engineering. A good example is germanium. Naturally, Ge is an indirect band gap material, but under just 2% tensile strain it is predicted to transform into a direct band gap semiconductor.[47] If we can create tensile-strained Ge QDs with a direct band gap, this would open up its use for optoelectronic applications.

Acknowledgements

This work was supported in part by the National Science Foundation under NSF CAREER Grant No. 1555270. PJS gratefully acknowledges the key contributions to this body of work by the members of his research group, particularly Christopher Schuck (Boise State University) [REF. 44], as well as the following key collaborators and their research groups: Christopher Yerino and Minjoo Larry Lee (Yale, UIUC) [REFS. 5, 6, 20, 21, 22, 23, 24, 43]; Baolai Liang and Diana Huffaker (UCLA) [REFS. 22, 23, 24, 43, 44]; Christian Schneider and Sven Höfling (Würzburg, St. Andrews) [REF. 24]; and Gregory Salamo (Arkansas) [REFS. 22, 23].

REFERENCES

[1] Huffaker, D. L., Park, G., Zou, Z., Shchekin, O. B. and Deppe, D. G., "1.3 μm room-temperature GaAs-based quantum-dot laser," Appl. Phys. Lett. **73**(18), 2564 (1998).

[2] Simmonds, P. J., Sun, M., Laghumavarapu, R. B., Liang, B., Norman, A. G., Luo, J.-W. and Huffaker, D. L., "Improved quantum dot stacking for intermediate band solar cells using strain compensation," Nanotechnology **25**(44), 445402 (2014).

[3] Leonard, D., Krishnamurthy, M., Reaves, C. M., Denbaars, S. P. and Petroff, P. M., "Direct formation of quantum-sized dots from uniform coherent islands of InGaAs on GaAs surfaces," Appl. Phys. Lett. **63**(23), 3203–3205 (1993).

[4] Eaglesham, D. J. and Cerullo, M., "Dislocation-free Stranski-Krastanow growth of Ge on Si(100)," Phys. Rev. Lett. **64**(16), 1943–1946 (1990).

[5] Simmonds, P. J. and Lee, M. L., "Tensile-strained growth on low-index GaAs," J. Appl. Phys. **112**, 54313 (2012).

[6] Lee, M. L. and Simmonds, P. J., "Tensile strained III-V self-assembled nanostructures on a (110) surface," Proc. SPIE **7768**, 776805 (2010).

[7] Tersoff, J. and LeGoues, F. K., "Competing relaxation mechanisms in strained layers," Phys. Rev. Lett. **72**(22), 3570 (1994).

[8] Schliwa, A., Winkelnkemper, M., Lochmann, A., Stock, E. and Bimberg, D., "In(Ga)As/GaAs quantum dots grown on a (111) surface as ideal sources of entangled photon pairs," Phys. Rev. B **80**(16), 161307(R) (2009).

[9] Adams, A., "Strained-layer quantum-well lasers," IEEE J. Sel. Top. Quantum Electron. **17**(5), 1364–1373 (2011).
[10] Belk, J. G., Sudijono, J. L., Yamaguchi, H., Zhang, X. M., Pashley, D. W., McConville, C. F., Jones, T. S. and Joyce, B. A., "Scanning tunneling microscopy studies of strain relaxation and misfit dislocations in InAs layers grown on GaAs(110) and GaAs(111)A," J. Vac. Sci. Technol. A **15**(3), 915 (1997).
[11] Wen, H., Wang, Z. M., Shultz, J. L., Liang, B. L. and Salamo, G. J., "Growth and characterization of InAs epitaxial layer on GaAs (111) B," article, Phys. Rev. B **70**(20), 205307 (2004).
[12] Pachinger, D., Groiss, H., Lichtenberger, H., Stangl, J., Hesser, G. and Schäffler, F., "Stranski-Krastanow growth of tensile strained Si islands on Ge (001)," Appl. Phys. Lett. **91**(23), 233106 (2007).
[13] Wasserman, D., Lyon, S. A., Hadjipanayi, M., Maciel, A. and Ryan, J. F., "Formation of self-assembled InAs quantum dots on (110) GaAs substrates," Appl. Phys. Lett. **83**(24), 5050 (2003).
[14] Stock, E., Warming, T., Ostapenko, I., Rodt, S., Schliwa, A., Töfflinger, J. A., Lochmann, A., Toropov, A. I., Moshchenko, S. A., Dmitriev, D. V., Haisler, V. A. and Bimberg, D., "Single-photon emission from InGaAs quantum dots grown on (111) GaAs," Appl. Phys. Lett. **96**, 93112 (2010).
[15] Treu, J., Schneider, C., Huggenberger, A., Braun, T., Reitzenstein, S., Höfling, S. and Kamp, M., "Substrate orientation dependent fine structure splitting of symmetric In(Ga)As/GaAs quantum dots," Appl. Phys. Lett. **101**, 22102 (2012).
[16] Juska, G., Murray, E., Dimastrodonato, V., Chung, T. H., Moroni, S. T., Gocalinska, A. and Pelucchi, E., "Conditions for entangled photon emission from (111)B site-controlled pyramidal quantum dots," J. Appl. Phys. **117**, 134302 (2015).
[17] Kulkova, I. V., Lyasota, A., Jarlov, C., Rigal, B., Rudra, A., Dwir, B. and Kapon, E., "Emission wavelength control of ordered arrays of InGaAs/GaAs quantum dots," J. Cryst. Growth **464**, 69–74 (2017).
[18] Lenz, A., Tournié, E., Schuppang, J., Dähne, M. and Eisele, H., "Atomic structure of tensile-strained GaAs/GaSb(001) nanostructures," Appl. Phys. Lett. **102**(10), 102105 (2013).
[19] Pohjola, P., Hakkarainen, T., Koskenvaara, H., Sopanen, M., Lipsanen, H. and Sainio, J., "Tensile-strained GaAsN quantum dots on InP," Appl. Phys. Lett. **90**(17), 172110 (2007).
[20] Toropov, A. A., Lyublinskaya, O. G., Meltser, B. Y., Solov'ev, V. A., Sitnikova, A. A., Nestoklon, M. O., Rykhova, O. V., Ivanov, S. V., Thonke, K. and Sauer, R., "Tensile-strained GaAs quantum wells and quantum dots in a GaAsxSb1-x matrix," Phys. Rev. B **70**(20), 205314 (2004).
[21] Simmonds, P. J. and Lee, M. L., "Tensile strained island growth at step-edges on GaAs(110)," Appl. Phys. Lett. **97**(15), 153101 (2010).
[22] Simmonds, P. J. and Lee, M. L., "Self-assembly on (111)-oriented III-V surfaces," Appl. Phys. Lett. **99**(12), 123111 (2011).
[23] Simmonds, P. J., Yerino, C. D., Sun, M., Liang, B., Huffaker, D. L., Dorogan, V. G., Mazur, Y., Salamo, G. and Lee, M. L., "Tuning Quantum Dot Luminescence Below the Bulk Band Gap Using Tensile Strain," ACS Nano **7**(6), 5017–5023 (2013).
[24] Yerino, C. D., Simmonds, P. J., Liang, B., Dorogan, V. G., Ware, M. E., Mazur, Y. I., Jung, D., Huffaker, D. L., Salamo, G. J. and Lee, M. L., "Tensile GaAs(111) quantum dashes with tunable luminescence below the bulk bandgap," Appl. Phys. Lett. **105**, 71912 (2014).
[25] Yerino, C. D., Simmonds, P. J., Liang, B., Jung, D., Schneider, C., Unsleber, S., Vo, M., Huffaker, D. L., Höfling, S., Kamp, M. and Lee, M. L., "Strain-driven growth of GaAs(111) quantum dots with low fine structure splitting," Appl. Phys. Lett. **105**(25), 251901 (2014).
[26] Ballingall, J. M. and Wood, C. E. C., "Crystal orientation dependence of silicon autocompensation in molecular beam epitaxial gallium arsenide," Appl. Phys. Lett. **41**(10), 947–949 (1982).
[27] Wang, W. I., "Instabilities of (110) III–V compounds grown by molecular beam epitaxy," J. Vac. Sci. Technol. B **1**, 630 (1983).
[28] Zhou, J., Huang, Y., Li, Y. and Jia, W. Y., "Growth and properties of AlGaAs/GaAs heterostructures on GaAs (110) surface," J. Cryst. Growth **81**, 221–223 (1987).
[29] Pfeiffer, L., West, K. W., Stormer, H. L., Eisenstein, J. P., Baldwin, K. W., Gershoni, D. and Spector, J., "Formation of a high quality two-dimensional electron gas on cleaved GaAs," article, Appl. Phys. Lett. **56**(17), 1697–1699 (1990).
[30] Wassermeier, M., Yang, H., Tournié, E., Däweritz, L. and Ploog, K., "Growth mechanism of GaAs on (110) GaAs studied by high-energy electron diffraction and atomic force microscopy," J. Vac. Sci. Technol. B **12**(4), 2574 (1994).

[31] Lee, J. H., Wang, Z. M., Kim, E. S., Kim, N. Y., Park, S. H. and Salamo, G. J., "Self-assembled InGaAs tandem nanostructures consisting of a hole and pyramid on GaAs (311)A by droplet epitaxy," Phys. Status Solidi A **207**, 348 (2010).
[32] Wang, Z. M., Liang, B. L., Sablon, K. A. and Salamo, G. J., "Nanoholes fabricated by self-assembled gallium nanodrill on GaAs(100)," Appl. Phys. Lett. **90**, 113120 (2007).
[33] Takebe, T., Fujii, M., Yamamoto, T., Fujita, K. and Watanabe, T., "Orientation-dependent Ga surface diffusion in molecular beam epitaxy of GaAs on GaAs patterned substrates," J. Appl. Phys. **81**(11), 7273 (1997).
[34] Barabási, A.-L., "Thermodynamic and kinetic mechanisms in self-assembled quantum dot formation," Mater. Sci. Eng. B **67**(1–2), 23–30 (1999).
[35] Yamamoto, T., Inai, M., Takebe, T. and Watanabe, T., "Pregrowth treatment dependence of surface morphology for GaAs grown on exactly oriented (111)A substrates by molecular-beam epitaxy," J. Vac. Sci. Technol. A **11**(3), 631–636 (1993).
[36] Sato, K., Fahy, M. R. and Joyce, B. A., "The growth of high quality GaAs on GaAs(111)A," Jpn. J. Appl. Phys. **33**, L905–L907 (1994).
[37] Joyce, B. A. and Vvedensky, D. D., "Self-organized growth on GaAs surfaces," Mater. Sci. Eng. R **46**(6), 127–176 (2004).
[38] Amar, J. G. and Family, F., "Critical Cluster Size: Island Morphology and Size Distribution in Submonolayer Epitaxial Growth," Phys. Rev. Lett. **74**(11), 2066–2069 (1995).
[39] Krzyzewski, T. J., Joyce, P. B., Bell, G. R. and Jones, T. S., "Scaling behavior in InAs/GaAs(001) quantum-dot formation," article, Phys. Rev. B **66**(20), 201302(R) (2002).
[40] Yang, K., Schowalter, L. J., Laurich, B. K., Campell, I. H. and Smith, D. L., "Molecular-beam epitaxy on exact and vicinal GaAs(ΙΤΤ) substrates," J. Vac. Sci. Technol. B **11**, 779 (1993).
[41] Houdré, R., Gueissaz, F., Gailhanou, M., Ganière, J., Rudra, A. and Ilegems, M., "Characterization of InGaAs and InAlAs layers on InP by four-crystal high resolution X-ray diffraction and wedge transmission electron microscopy," J. Cryst. Growth **111**, 456–460 (1991).
[42] Brown, A. S., Metzger, R. A. and Henige, J. A., "Growth and properties of AlInAs–GaInAs alloys and quantum wells on (110) InP," J. Vac. Sci. Technol. B **11**(3), 817–819 (1993).
[43] Yasuda, Y., Koh, S., Ikeda, K. and Kawaguchi, H., "Crystal growth of InGaAs/InAlAs quantum wells on InP(110) by MBE," J. Cryst. Growth **364**, 95–100 (2013).
[44] Yerino, C. D., Liang, B., Huffaker, D. L., Simmonds, P. J. and Lee, M. L., "Review Article: Molecular beam epitaxy of lattice-matched InAlAs and InGaAs layers on InP(111)A, (111)B, and (110)," J. Vac. Sci. Technol. B **35**, 10801 (2017).
[45] Schuck, C. F., McCown, R. A., Hush, A., Mello, A., Roy, S., Spinuzzi, J. W., Liang, B., Huffaker, D. L. and Simmonds, P. J., "Self-assembly of (111)-oriented tensile-strained quantum dots by molecular beam epitaxy," J. Vac. Sci. Technol. B, in review (2018).
[46] Yeo, W., Dimitrov, R., Schaff, W. J. and Eastman, L. F., "Material properties of bulk InGaAs and InAlAs/InGaAs heterostructures grown on (111)B and (111)B misoriented by 1° towards ⟨211⟩ InP substrates," Appl. Phys. Lett. **77**(26), 4292 (2000).
[47] El Kurdi, M., Fishman, G., Sauvage, S. and Boucaud, P., "Band structure and optical gain of tensile-strained germanium based on a 30 band k · p formalism," J. Appl. Phys. **107**(1), 13710 (2010).